JOURNAL OF Materials CHEMISTRY

A new cointercalated superconducting bismuth cuprate, $(HgI_2)_{0.5}I_{0.5}Bi_{1.85}Pb_{0.35}Sr_{1.9}Ca_{2.1}Cu_{3.1}O_{10+\delta}$

Jin-Ho Choy,* Woo Lee and Seong-Ju Hwang

National Nanohybrid Materials Laboratory, School of Chemistry and Molecular Engineering, Seoul National University, Seoul 151-742, Korea. Tel: +82-2-880-6658; Fax: +82-2-872-9864; E-mail: jhchoy@plaza.snu.ac.kr

Received 14th February 2000, Accepted 20th April 2000
Published on the Web 20th June 2000

Intercalation of HgI_2 into high-T_c superconducting $Bi_{1.85}Pb_{0.35}Sr_{1.9}Ca_{2.1}Cu_{3.1}O_{10+\delta}$ (Bi2223) compound is achieved by a stepwise reaction technique in which the iodine intercalate is used as a secondary host material. While the vapor transport reaction is ineffective in intercalating mercuric salts directly into Pb-doped or single crystalline Bi-based cuprates, the present stepwise reaction method can provide a useful way of intercalating larger molecules into Bi_2O_2 double layers of Bi-based cuprates. According to Hg L_{III}-edge extended X-ray absorption fine structure analyses, it is found that the intercalated mercuric iodide is stabilized as a linear molecule with additional free iodine species in the interlayer space of Bi2223. Taking into account the fact that no free iodine can be found in the HgI_2 intercalated $Bi_2Sr_2CaCu_2O_{8+\delta}$ polycrystal prepared by the direct intercalation method, the present experimental finding indicates that the intracrystalline structure of mercuric iodides in Bi_2O_2 double layers can be modified by controlling the synthetic route. The linear geometry of intercalated mercuric iodide has been further confirmed by performing *ex-situ* X-ray diffraction measurements on the deintercalation products, which clarify that the partial deintercalation of mercuric iodide leads to the formation of an intermediate phase with a parallel orientation of HgI_2 molecules with respect to the basal plane.

Introduction

Since the intercalation reaction provides a way of preparing novel compounds with self-assembled multi-layer structures by hybridizing various kinds of chemical species with two dimensional host lattices, new superconducting heterostructures and nanodevices can be explored by applying this technique to high-T_c superconducting layered oxides such as Bi-based cuprates, $Bi_2Sr_2Ca_{n-1}Cu_nO_{2n+4+\delta}$ (hereafter will be referred to be Bi2201 for $n=1$, Bi2212 for $n=2$, and (Bi,Pb)2223 for $n=3$, respectively). With this technique, we have synthesized successfully a series of superconducting oxide–halogenide (inorganic–inorganic) nanohybrids, M–X–$Bi_2Sr_2Ca_{n-1}Cu_nO_{2n+4+\delta}$ (M = Hg, Ag, and Au; X = Br and I; $n=1$ and 2) and covalent–ionic (organic–inorganic) nanohybrids, $[Py–C_xH_{2x+1}I]_2HgI_4–Bi_2Sr_2Ca_{n-1}Cu_nO_{2n+4+\delta}$ (Py = pyridine; $n=1$ and 2), which are based on the hard–soft–acid–base (HSAB) concept and the interlayer complexation method, respectively.[1–7] According to the X-ray diffraction (XRD) and magnetic susceptibility measurements, all these compounds are found to be superconducting with slightly lowered T_c ($\Delta T_c = -5$ to -7 K) for the former or even slightly higher T_c's ($\Delta T_c = 1$–0 K) for the latter, compared to the pristine material ($T_c = 81$ K for $n=2$), although they show remarkable basal increments upon intercalation ($\Delta d = 6$–7 Å for the former and $\Delta d = 11$–31 Å for the latter). From the viewpoint of practical applications, these superconducting nanohybrids are available as electrodes in various electrochemical devices and fast switching devices, since they possess a spectrum of transport properties extending from insulating–superconducting to superionic–superconducting or superionic–normal metallic. Furthermore, it was also demonstrated that superconducting thin films or nano-particles could be realized highly economically by separating each superconducting block through the intercalation of bulky organic molecules.[8] Such results have encouraged us to extend our research to (Bi,Pb)2223, because this phase has the highest T_c of ≈ 110 K and the greatest current density of $J_{c(70\ K,\ 0\ T)} = \approx 10^6$ A cm^{-2} among the Bi-based cuprates.[9] However, in contrast to Bi2201 and Bi2212, an attempt to intercalate metal halides into the (Bi,Pb)2223 lattice proved to be unsuccessful, which is ascribed not only to its poor capability for elastic deformation upon intercalation, but also to its larger interactive force in between the Bi_2O_2 double layers enhanced by the substitution of Bi^{3+} with Pb^{2+}.[10]

In this work, we have prepared for the first time the high-T_c superconducting HgI_2–(Bi,Pb)2223 nanohybrid by adopting a stepwise synthetic method where the iodine intercalate is used as a secondary host material. The effect of reaction conditions on the intracrystalline structure of the mercuric iodide layers has been examined by performing extended X-ray absorption fine structure (EXAFS) studies as well as one-dimensional electron density calculations. An *ex-situ* XRD measurement on the deintercalated phase was also carried out to investigate the variation of the interlayer structure upon deintercalation.

Experimental

A polycrystalline sample of (Bi,Pb)2223 was prepared by the conventional solid state reaction. At first, the powder reagents of Bi_2O_3, PbO, $SrCO_3$, $CaCO_3$, and CuO were thoroughly mixed with molar ratios of Bi : Pb : Sr : Ca : Cu = 1.85 : 0.35 : 1.9 : 2.1 : 3.1 and then calcined at 775 °C for 24 h in air. This pre-fired material was pressed into 13 mm disk-shaped pellets, sintered at 840 °C for 126 h with some intermittent grindings, and finally quenched to room temperature.

The intercalation of HgI_2 into (Bi,Pb)2223 was achieved by a stepwise reaction scheme as follows. At first, the iodine intercalated (Bi,Pb)2223 compound (hereafter referred to as I(Bi,Pb)2223) was obtained by heating the vacuum sealed tube containing the pristine (Bi,Pb)2223 with five equivalent of iodine per formula unit of host.[11] Secondly, the intercalation of

DOI: 10.1039/b001195i

HgI_2 was carried out by reacting I(Bi,Pb)2223 and HgI_2 (mole ratio of 1 : 5) in a Pyrex tube, one end of which was open to the air, at 253 °C for 24 h. To facilitate HgI_2 intercalation, one mole of free iodine as transporting agent was introduced into the tube.

The formation of single phase (Bi,Pb)2223 and its iodine and HgI_2 intercalates were checked out by XRD analysis using a Phillips PW3710 powder diffractometer equipped with Ni-filtered Cu-K_α radiation ($\lambda_{\alpha1} = 1.5406$ Å). The effect of intercalation on the superconductivity was examined by measuring the AC magnetic susceptibility (χ_{ac}) with an Oxford Maglab system in an alternating applied field of 20 mOe ($f = 330$ Hz). The amount of guest species introduced into the host lattice was estimated by performing thermogravimetric analyses (TGA) in the temperature range of 20–800 °C using a DuPont 2000 thermal analysis station. The sample was heated at a rate of 10 °C min^{-1} under ambient atmosphere. As shown in Fig. 1, the intercalated mercuric iodide is completely deintercalated below 500 °C, suggestive of a weak interaction between the host lattice and the guest molecule. The total weight loss was determined to be 22.0%, which is in good agreement with the calculated value (21.4%) of $(HgI_2)_{0.5}I_{0.5}$-$Bi_{1.85}Pb_{0.35}Sr_{1.9}Ca_{2.1}Cu_{3.1}O_{10}$ (hereafter referred to as $(HgI_2)_{0.5}I_{0.5}$(Bi,Pb)2223). The stoichiometry obtained from TGA was cross-confirmed by electron probe microanalysis (EPMA) which was carried out using a JEOL JXA-8600 X-ray analyzer with a 100 µm diameter probe at 20.0 kV and 5.5×10^{-9} A. The observed weight percentages of each element in the pristine (Bi,Pb)2223 and its HgI_2 intercalate are listed in Table 1, together with the calculated values. The X-ray absorption spectra (XAS) were measured with the EXAFS facility installed at the beam line 10B at the Photon Factory (Tsukuba), which was operated at 2.5 GeV and 260–370 mA.[12] The samples were finely ground, mixed with dry boron nitride (BN) in an appropriate ratio, and pressed into pellets in order to get an optimum absorption jump ($\Delta\mu t \approx 1$) enough to be free from the thickness and pin-hole effects.[13] All the present spectra were collected in transmission mode using gas-ionization detectors.

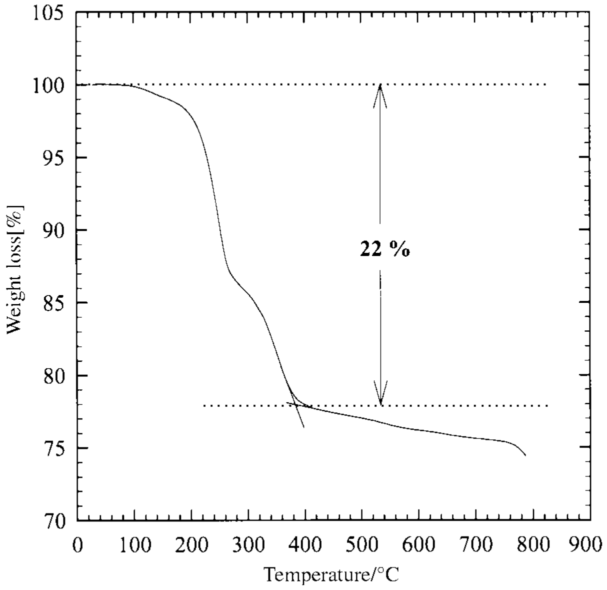

Fig. 1 Thermogravimetric curve for the HgI_2 intercalated (Bi,Pb)2223. The sample was heated in ambient atmosphere at rate of 10 °C min^{-1}.

Results and discussion

Intercalation reactions under various conditions

In order to probe the main factors in intercalating HgI_2 into the Bi-based cuprates, various kinds of reactions were performed with different host compounds and dissimilar reaction routes, as summarized in Table 2. From these results, it becomes certain that $(HgI_2)_{0.5}I_{0.5}$(Bi,Pb)2223 can be reproducibly prepared only by the stepwise intercalation route with a secondary host of I(Bi,Pb)2223. This is surely attributed not only to the poorer capability of the host (Bi,Pb)2223 lattice for a large elastic deformation due to its thicker unit block containing three CuO_2 layers, but also to an enhanced attraction between Bi_2O_2 double layers due to the substitution of Bi^{3+} ion with Pb^{2+}.[10] The former effect also plays a significant role in the synthesis of HgI_2 intercalated Bi2212 (hereafter referred to as $(HgI_2)_{0.5}$Bi2212) single crystals, since it can not be obtained through direct intercalation methods. Such a difficulty can be overcome by using the stepwise intercalation route, because it is much easier to intercalate the bulky HgI_2 molecule into the expanded interlayer space of the iodine intercalate compared to that of the pristine compound. The direct intercalation method is also revealed to be unsuccessful in intercalating HgI_2 into Pb-substituted Bi2212, even though it has a thinner unit block with two CuO_2 layers than (Bi,Pb)2223. This is surely attributed to the second effect of Pb substitution.[10] Also for this case, the iodine molecule can be easily intercalated into the host lattice due to its smaller molecular size, which gives rise to the reduction of the attractive interaction between $(Bi,Pb)_2O_2$ double layers. Then, larger HgI_2 molecules can be further intercalated into the interlayer space of I(Bi,Pb)2212. On the other hand, it is worthy to note here that the stepwise reaction in a sealed tube does not lead to the formation of the HgI_2 intercalate of Bi2212 single crystals or Pb-doped Bi-based cuprates, in contrast to the reaction in air. This implies a possible role of oxygen in the intercalation process and/or a need for partial deintercalation of the pre-intercalated iodine. Between both possibilities, the

Table 1 Observed and calculated weight percentages of each element in (Bi,Pb)2223 and $(HgI_2)_{0.5}I_{0.5}$(Bi,Pb)2223

	(Bi,Pb)2223		$(HgI_2)_{0.5}I_{0.5}$(Bi,Pb)2223	
Element	wt.% (obs.)[a]	wt.% (calc.)[b]	wt.% (obs.)[a]	wt.% (calc.)[b]
Hg	—	—	7.72	7.39
I	—	—	14.24	14.02
Bi	36.34	36.24	28.59	28.48
Pb	6.71	6.80	5.49	5.34
Sr	14.82	15.61	11.95	12.26
Ca	7.63	7.89	6.21	6.20
Cu	18.75	18.47	13.97	14.51
O[c]	15.75	15.00	11.83	11.79

[a]The observed values are obtained by averaging the data of three independent EPMA measurements for each sample. [b]The theoretical values are calculated with the nominal compositions of $Bi_{1.85}Pb_{0.35}Ca_{1.9}Sr_{2.1}Cu_{3.1}O_y$ for the pristine compound and $(HgI_2)_{0.5}I_{0.5}Bi_{1.85}Pb_{0.35}Ca_{1.9}Sr_{2.1}$-$Cu_{3.1}O_y$ for the mercuric iodide intercalate. [c]The oxygen contents are estimated by subtracting the sum of weight percentages for other elements from one hundred percent.

former is excluded completely from the fact that the HgI_2 intercalate can also be prepared in an N_2 atmosphere. Therefore, it is concluded that, in order to complete the HgI_2 intercalation *via* the stepwise method, a fraction of the pre-intercalated iodine should be deintercalated to provide sufficient interlayer space for the diffusion of bulky HgI_2 molecules.

Powder XRD analysis

The powder XRD patterns for the pristine (Bi,Pb)2223 and its iodine and mercuric iodide intercalates are shown in Figs. 2a–c, respectively. Upon intercalation of iodine and mercuric iodide, all the (00*l*) reflections are shifted toward lower angles, indicating the formation of single phasic intercalates with larger basal spacings. From the least squares fitting analyses, the *c*-axis unit cell parameter for the pristine compound is determined to be 18.48_9 Å, while those for the iodine and HgI_2 intercalates are estimated to be 21.93_0 and 25.24_6 Å, respectively, as listed in Table 3. Since there are two intercalant layers for each unit cell of (Bi,Pb)2223, the basal increment for each guest layer is calculated to be 3.44_1 Å for I(Bi,Pb)2223 and 6.75_7 Å for $(HgI_2)_{0.5}I_{0.5}$(Bi,Pb)2223. Such results show that the lattice expansions for iodine and mercuric iodide intercalated (Bi,Pb)2223 are slightly smaller than those for the corresponding Bi2212 homologues,[2] which might be attributed to the stronger interlayer attraction between (Bi,Pb)O layers in the former. It is also observed that the (00*l*) peaks of the intercalates are rather broader than those of the pristine compound, indicating the decrease of crystallinity caused by the severe elastic deformation of the host lattice during the intercalation process. On the other hand, the XRD pattern for the deintercalated product of $(HgI_2)_{0.5}I_{0.5}$(Bi,Pb)2223 was also measured to check out the reversibility of the HgI_2 intercalation. As shown in Fig. 2d, the pristine (Bi,Pb)2223 phase is restored by heating the HgI_2 intercalate at 500 °C for 1 h, clarifying the reversibility of the intercalation reaction.

AC magnetic susceptibility measurements

Fig. 3 represents the AC magnetic susceptibilities for pristine (Bi,Pb)2223, and its iodine and mercuric iodide intercalates as a function of temperature. Both the intercalates exhibit superconducting transitions at 97 K for I(Bi,Pb)2223 and at 96 K for $(HgI_2)_{0.5}I_{0.5}$(Bi,Pb)2223, which are slightly lower than that for the pristine (Bi,Pb)2223 ($\approx$104 K). In contrast to the intercalates, the pristine compound shows a two-step superconducting transition, which originates from the bulk phase and the Josephson-like weak link between the grains, not from the inhomogeneity of the sample.[14] In this context, complete disappearance of the two-step transition for both intercalates can be understood as a result of elimination of the weak link due to the intercalation of iodine and HgI_2. On the other hand, it is noteworthy that the superconducting transition temperature drops only by a small fraction (7 K for 3.44_1 Å and 8 K for 6.75_7 Å for iodine and mercuric iodide intercalates, respectively), in spite of the remarkable lattice expansion upon intercalation. This indicates that the effect of interblock electronic coupling would be negligible in the present (Bi,Pb)2223 system, which is consistent with our previous studies on the metal salt intercalated Bi2212 system.[1–6]

Table 2 Effect of reaction conditions on the formation of the HgI_2 intercalation compound

	Direct method	Stepwise method		
Host material	Vacuum	Vacuum	Air	N_2
Bi2212 polycrystal	○[a]	○	○	○
Bi2212 single crystal	×[a]	×	○	○
(Bi,Pb)2212 polycrystal	×	×	○	○
(Bi,Pb)2223 polycrystal	×	×	○	○

[a]The circle and cross symbols represent successful and failed HgI_2 intercalation, respectively.

Hg L_{III}-edge EXAFS analysis

In order to investigate the effect of the intercalation conditions on the intracrystalline structure of the mercuric iodide layers, comparative Hg L_{III}-edge EXAFS analyses were performed for $(HgI_2)_{0.5}I_{0.5}$(Bi,Pb)2223 (prepared by the stepwise intercalation method) and $(HgI_2)_{0.5}$Bi2212 (prepared by the direct intercalation method). The k^3-weighted Hg L_{III}-edge EXAFS spectra for $(HgI_2)_{0.5}I_{0.5}$(Bi,Pb)2223 and $(HgI_2)_{0.5}$Bi2212 are shown in Fig. 4a, in comparison with that for the unintercalated free HgI_2. The corresponding Fourier transforms (FTs) in the k range of 1.5–11.9 $Å^{-1}$ are represented in Fig. 4b. A doubly split FT peak is discernible at around 2.0 and 2.6 Å for all the present compounds. Such a peak splitting is attributed to the Ramsauer–Townsend resonance which occurs generally in the backscattering amplitude of heavy atoms with high atomic numbers.[15] Since the first peak in the FT corresponds to the mercury–iodine bonding pair, it was inversely Fourier transformed to k space for curve fitting analyses in order to determine the structural parameters such as coordination number (CN), bond length (R_{Hg-I}), and Debye–Waller factor (σ^2). The resulting $k^3\chi(k)$ Fourier filtered EXAFS oscillations are plotted in Fig. 5. The amplitude of EXAFS oscillation for the free HgI_2 is found to be depressed uniformly over the entire k range upon intercalation, indicating a decrease in coordination number.[16] It is also observed that the oscillation frequencies for both HgI_2 intercalates decrease commonly compared to that for free HgI_2, which implies that the mercury–iodine bond distance becomes remarkably shorter upon intercalation. The best fitting results to the first coordination shell are compared to the experimental spectra in Figs. 4b and 5 and the fitted structural parameters are summarized in Table 4. Since the coordination number obtained from the fitting analysis corresponds to the product ($S_0^2 \times$CN) of coordination number (CN) and amplitude reduction factor (S_0^2),[16] it is possible to determine the exact coordination number of the mercuric iodide intercalate by knowing the amplitude reduction factor for a specific

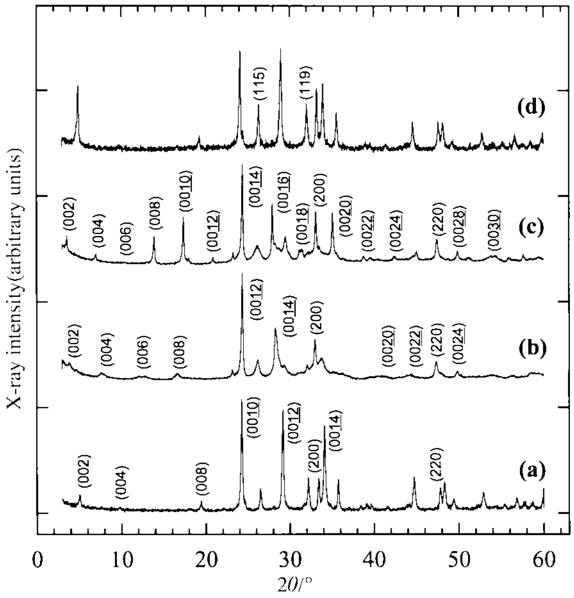

Fig. 2 Powder XRD patterns for (a) pristine (Bi,Pb)2223, (b) I(Bi,Pb)2223, (c) $(HgI_2)_{0.5}I_{0.5}$(Bi,Pb)2223, and (d) the deintercalation product of $(HgI_2)_{0.5}I_{0.5}$(Bi,Pb)2223 after heat treatment at 500 °C for 1 h. All the reflections could be indexed on the basis of the double-slab tetragonal unit cell.

Table 3 Basal spacing (c), lattice expansion upon intercalation (Δc), and superconducting transition temperature (T_c) for pristine (Bi,Pb)2223 and its iodine and mercuric iodide intercalates

Compound	c/Å	Δc/Å	T_c/K
(Bi,Pb)2223	18.48_9[a]	—	104
I(Bi,Pb)2223	21.93_0	3.44_1	97
$(HgI_2)_{0.5}I_{0.5}$(Bi,Pb)2223	25.24_6	6.75_7	96

[a] This value is the half of the unit cell parameter of (Bi,Pb)2223.

absorber–scatterer pair of (Hg–I). In the present analysis, the amplitude reduction factor obtained from the free HgI_2 reference (0.72_1) was used to calculate the coordination number of mercury in the HgI_2 intercalates. As listed in Table 4, the mercury in $(HgI_2)_{0.5}$Bi2212 is revealed to be coordinated with two iodine atoms as in the vapor state.[2] However, the coordination number of mercury in $(HgI_2)_{0.5}I_{0.5}$ (Bi,Pb)2223 is determined to be 2.50, which is somewhat higher than that in $(HgI_2)_{0.5}$Bi2212. Such a finding suggests the existence of some iodine species in the (Bi,Pb)–O double layers of $(HgI_2)_{0.5}I_{0.5}$(Bi,Pb)2223, as proposed from the EPMA and TGA results. In order to check out the possibility of additional iodine species in the interlayer space of the Bi_2O_2 double layers, the volume demand of mercuric iodide molecule was calculated as follows. Based on the length of the linear HgI_2 molecule ($\approx$9.5 Å) and the van der Waals diameter of I_2 ($\approx$4 Å), the volume of the guest HgI_2 molecule in the Bi_2O_2 double layer is roughly estimated to be $\approx$125 Å^3. Since the total gallery space is calculated to be $\approx$197 Å^3 per guest molecule, there is a free gallery space of $\approx$72 Å^3, which is large enough to accommodate an additional iodine molecule (the volume of which is about 42 Å^3). In spite of the presence of additional iodine species, our recent micro-Raman study, which will be published elsewhere, reveals that the mercury atom is coordinated with two iodine atoms to form a linear HgI_2 molecule. While three Raman peaks should be detected for trigonal (or square) planar symmetry, only one phonon line is discernible at 130 cm^{-1} for $(HgI_2)_{0.5}I_{0.5}$(Bi,Pb)2223, indicating the linear symmetry of the intercalated mercuric iodide. In this regard, it can be concluded that there are two kinds of guest molecules in the interlayer space for the present (Bi,Pb)2223 compound, namely a linear HgI_2 molecule and an uncoordinated additional free iodine. Taking into account that HgI_2-intercalated Bi2212 and (Bi,Pb)2223 compounds are prepared *via* different intercalation routes, the observed inconsistency of Hg coordination number for both intercalates is surely ascribed to their dissimilar synthetic conditions. In this context, the existence of free iodine in $(HgI_2)_{0.5}I_{0.5}$(Bi,Pb)2223 can be reasonably understood from the fact that the iodine intercalate is used as a secondary host material. Since the pre-intercalated iodine species would not be wholly deintercalated during the second step of the stepwise intercalation reaction, it can exist as free iodine in the interlayer space. In fact, it has been reported that, in various intercalation systems,[17] a small amount of additional transporting agent is still trapped in the interlayer space of the host together with the guest molecules.

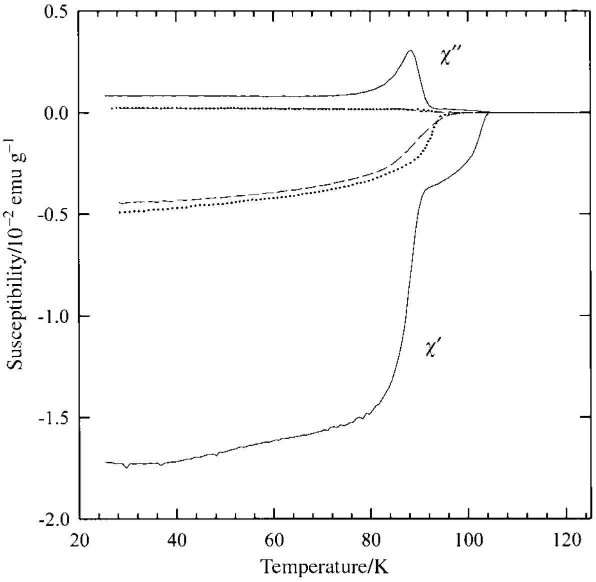

Fig. 3 Temperature dependence of the real (χ′) and imaginary (χ″) parts of the AC susceptibilities for pristine (Bi,Pb)2223 (solid lines), I(Bi,Pb)2223 (dotted lines), and $(HgI_2)_{0.5}I_{0.5}$(Bi,Pb)2223 (dashed lines). While the pristine sample is disk-shaped, the corresponding intercalates are powdered.

One-dimensional electron density calculations

For the purpose of confirming the presence of additional iodine in HgI_2 intercalated (Bi,Pb)2223, we calculated the one dimensional electron density along the z-direction, $\rho(z)$, on the basis of the (00l) reflection intensities (Fig. 6a). Alternatively, we have obtained the other Fourier map from the suggested crystal structure where the intercalated HgI_2 is stabilized as a linear molecule together with an additional iodine species. As shown in Fig. 6a, there is a good agreement between the electron density maps, clarifying the fitness of the present intracrystalline structural model. From the present electron density calculation, the tilting angle of the guest HgI_2 molecule is estimated to be $\approx$50.5° with respect to the c-axis.[18]

Ex-situ XRD measurements on the deintercalation product

The evolution of crystal structure upon deintercalation has also been examined by performing XRD analysis for the deinterca-

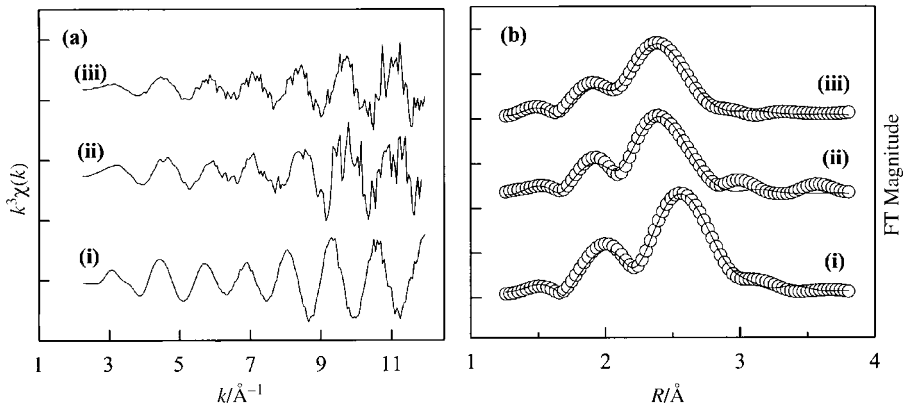

Fig. 4 (a) Experimental k^3-weighted Hg L_{III}-edge EXAFS spectra and (b) corresponding Fourier transforms of (i) HgI_2, (ii) $(HgI_2)_{0.5}I_{0.5}$(Bi,Pb)2223, and (iii) $(HgI_2)_{0.5}$Bi2212. The solid lines and empty circles represent the fitted and experimental data, respectively.

Table 4 Results of non-linear least squares curve fitting for the first shell of Hg L_{III}-edge EXAFS spectra

	Parameters			
Compound	R_{Hg-I}/Å	CN	$\sigma^2/\times10^{-3}$ Å^2	F^b
HgI_2	2.76_5	4^a	7.26	0.025
$(HgI_2)_{0.5}I_{0.5}$(Bi,Pb)2223	2.64_5	2.5_0	7.53	0.030
$(HgI_2)_{0.5}$Bi2212	2.64_5	1.9_2	6.24	0.036

[a]The coordination number (CN) of the reference HgI_2 was fixed to the crystallographic value in order to determine the amplitude reduction factor. The fitting analysis was carried out for the first shell of the HgI_4 tetrahedron. [b]The reliability of the fit was evaluated by the F factor, $F=[\sum_i k^6\{\chi_i(k)_{exp.}-\chi_i(k)_{fit}\}^2/(N-1)]^{1/2}$, where N is the number of data points.

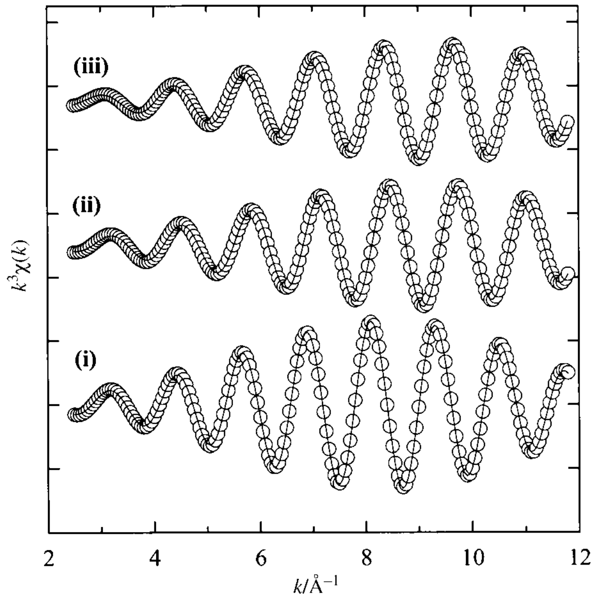

Fig. 5 Fourier filtered Hg L_{III}-edge EXAFS spectra of (i) HgI_2, (ii) $(HgI_2)_{0.5}I_{0.5}$(Bi,Pb)2223, and (iii) $(HgI_2)_{0.5}$Bi2212. The solid lines and empty circles represent the fitted and experimental data, respectively.

lated phase of $(HgI_2)_{0.5}I_{0.5}$(Bi,Pb)2223 with a weight loss of ≈15%.[19] As shown in Fig. 7, a new series of (00*l*) reflection peaks appears in the present XRD pattern. From the non-linear least squares fitting, the *c*-axis unit cell parameter of this new phase is determined to be 22.07 Å, which is markedly shorter than that of the fully HgI_2 loaded phase (25.25 Å). Such a lattice contraction during the deintercalation process is attributed to a change in the intracrystalline structure of mercuric iodide, in which the tilted orientation of the linear mercuric iodide molecule is changed to an orientation parallel to the *ab* plane. This is due to the fact that the close-packing of linear HgI_2 molecules can not be maintained with decreasing guest content. In this regard, the formation of an intermediate phase upon deintercalation can be regarded as further evidence

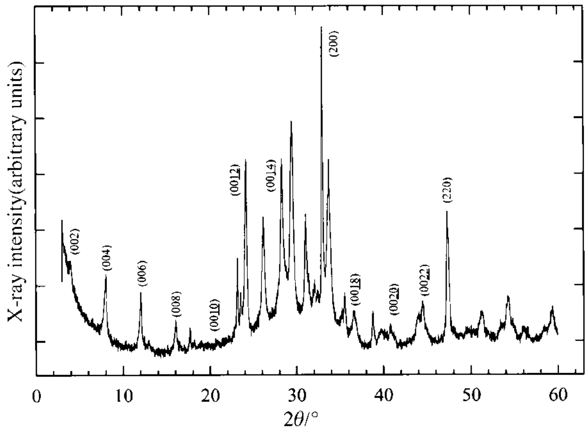

Fig. 7 Powder XRD pattern of the deintercalation product of $(HgI_2)_{0.5}I_{0.5}$(Bi,Pb)2223 with a weight loss of ≈15%. The sample was heated at 300 °C in a constant temperature furnace. After the heat treatment, the weight loss was checked gravimetrically by using a balance with an accuracy of 10^{-1} mg.

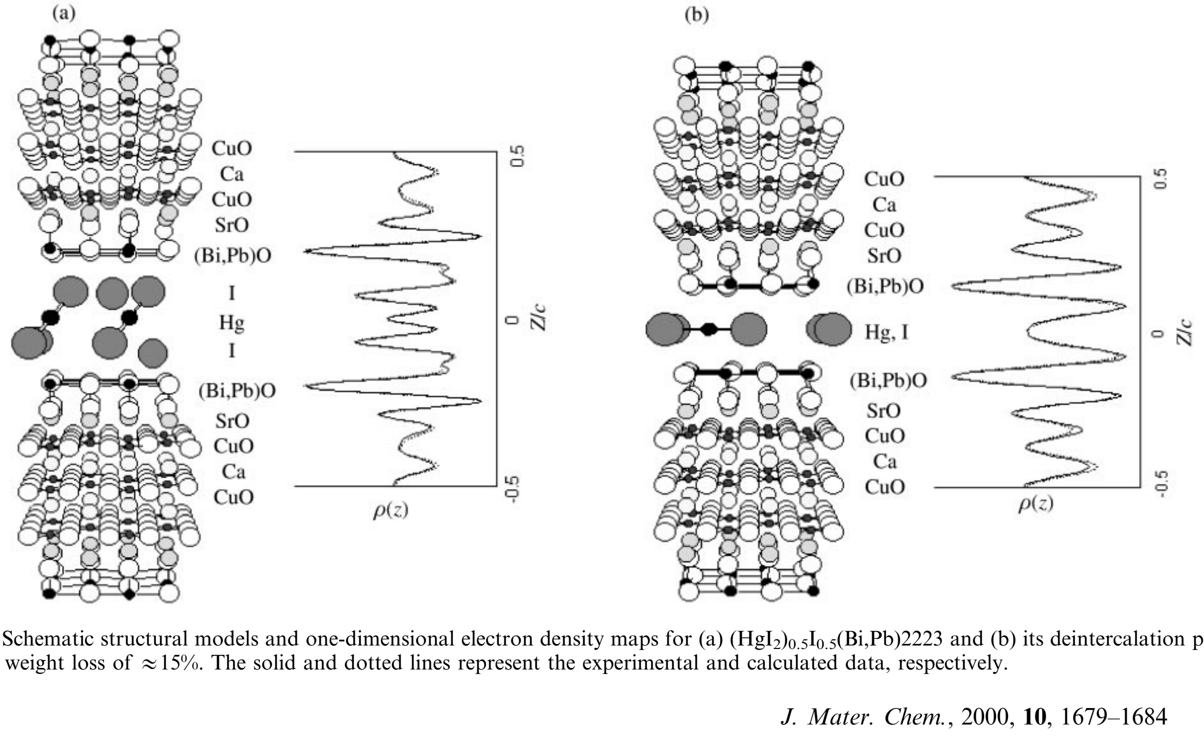

Fig. 6 Schematic structural models and one-dimensional electron density maps for (a) $(HgI_2)_{0.5}I_{0.5}$(Bi,Pb)2223 and (b) its deintercalation product with a weight loss of ≈15%. The solid and dotted lines represent the experimental and calculated data, respectively.

for the presence of linear mercuric halide molecules. In order to identify the crystal structure of this intermediate phase, a one dimensional electron density map was also calculated based on this structural model. As can be seen from Fig. 6b, there is excellent consistency between the observed electron density and the calculated one, indicative of the correctness of the present structure. On the basis of this experimental finding, the stepwise weight decrease in the TGA can be attributed to the change in configuration of the linear HgI_2 molecules upon heating. To our knowledge, this is the first example of a structural phase transition induced by deintercalation of an inorganic intercalant, although such a phenomenon has been well known for organic molecule intercalation compounds.[20–24]

Conclusion

In this study, we have developed a new stepwise intercalation route for the intercalation of mercuric iodide into (Bi,Pb)2223 superconductor. The present stepwise reaction method is expected to be available as an alternative way of intercalating larger molecules into Bi_2O_2 double layers of Pb-doped or single crystalline Bi-based cuprates with a strong attractive interlayer interaction and/or a poor capability for elastic deformation. According to the Hg L_{III}-edge EXAFS analyses and one-dimensional electron density calculations on the HgI_2 intercalated (Bi,Pb)2223, it is found that the intercalated mercuric iodide is stabilized as a linear molecule with additional free iodine species in the interlayer space of the Bi_2O_2 double layer. Considering the fact that there is no additional iodine in the HgI_2 intercalated Bi2212 prepared by the direct intercalation method, it is concluded that the intracrystalline structure of the mercuric iodide layers can be modified by controlling the synthetic conditions. The presence of linear mercuric iodide molecules in HgI_2 intercalated (Bi,Pb)2223 is further evidenced from the *ex-situ* XRD study on the deintercalation product, which reveals the formation of a new intermediate phase with HgI_2 molecules oriented parallel to the basal plane. This is the first example of a structural phase transition caused by deintercalation of inorganic guest species.

Acknowledgements

This work was supported in part by the Ministry of Education (BSRI-98-3413) and by the Korean Science and Engineering Foundation through the Center for Molecular Catalysis. Authors are grateful to Prof. M. Nomura for helping us to get the XAS data at the Photon Factory. W. Lee wants to express his thanks for the BK21 fellowship.

References

1 J. H. Choy, N. G. Park, S. J. Hwang, D. H. Kim and N. H. Hur, *J. Am. Chem. Soc.*, 1994, **116**, 11564.
2 J. H. Choy, S. J. Hwang and N. G. Park, *J. Am. Chem. Soc.*, 1997, **119**, 1624.
3 J. H. Choy, S. J. Hwang and D. K. Kim, *Phys. Rev. B*, 1997, **55**, 5674.
4 J. H. Choy, N. G. Park, Y. I. Kim, S. H. Hwang, J. S. Lee and H. I. Yoo, *J. Phys. Chem.*, 1995, **99**, 7845.
5 M. K. Bae, M. S. Kim, S. I. Lee, N. G. Park, S. J. Hwang, D. H. Kim and J. H. Choy, *Phys. Rev. B*, 1996, **53**, 12416.
6 J. H. Choy, N. G. Park, S. J. Hwang and Z. G. Kim, *J. Phys. Chem.*, 1996, **100**, 3783.
7 J. H. Choy, S. J. Kwon and G. S. Park, *Science*, 1998, **280**, 1589.
8 J. H. Choy, S. J. Kwon, S. J. Hwang, Y. I. Kim and W. Lee, *J. Mater. Chem.*, 1999, **9**, 129.
9 A. Jeremie, K. Alami-Yadri, J. C. Grivel and R. Flukiger, *Supercond. Sci. Technol.*, 1993, **6**, 730.
10 (*a*) C. S. Gopinath and S. Subramanian, *Physica C*, 1991, **176**, 331; (*b*) G. Calestani, M. G. Francesconi, G. Salsi, G. D. Andreetti and A. Migliori, *Physica C*, 1993, **197**, 283.
11 J. H. Choy, S. J. Hwang and W. Lee, *J. Solid State Chem.*, 1999, **142**, 199.
12 (*a*) H. Oyanagi, T. Matsushida, M. Ito and H. Kuroda, *KEK Report*, 1984, **83**, 30; (*b*) H. Kuroda and A. Koyama, *KEK Report*, 1985, **84**, 19.
13 (*a*) F. W. Lytle, G. van der Laan, R. B. Greegor, E. M. Larson, C. E. Violet and J. Wong, *Phys. Rev. B*, 1990, **41**, 8955; (*b*) E.-A. Stern and K. Kim, *Phys. Rev. B*, 1981, **23**, 3781.
14 H. Mazaki, M. Takano, J. Takada, K. Oda, H. Kitaguchi, Y. Miura, Y. Ikeda, Y. Tomii and T. Kubozoe, *Jpn. J. Appl. Phys.*, 1988, **27**, L1639 and references therein.
15 N.-F. Mott and H.-S.-W. Massey, *The Theory of Atomic Collisions*, Clarendon Press, Oxford, 1995.
16 B. K. Teo, *EXAFS: Basic Principles and Data Analysis*, Springer-Verlag, Berlin, 1986.
17 E. Stumpp, *Mater. Sci. Eng.*, 1977, **31**, 53 and references therein.
18 In the case of $(HgI_2)_{0.5}$Bi2212, the HgI_2 molecular axis is found to be tilted at an angle of $\approx 48°$ with respect to the *c*-axis (see ref. 1), which is smaller than the tilting angle for the present $(HgI_2)_{0.5}I_{0.5}$(Bi,Pb)2223. Such a small tilting angle in the former represents a larger interlayer distance.
19 As can be seen from Fig. 1, there is a remarkable slope change in the TGA curve near 300 °C, corresponding to a weight decrease of $\approx 15\%$. In order to probe the origin of the steps in the TGA curve, we have prepared a deintercalation product with a weight loss of $\approx 15\%$.
20 M. B. Dines, *Inorg. Chem.*, 1978, **17**, 173.
21 A. Weiss and R. Ruthardt, *Z. Naturforsch., Teil B*, 1969, **24**, 355.
22 A. Weiss and R. Ruthardt, *Z. Naturforsch., Teil B*, 1969, **24**, 1066.
23 R. Schollhorn, E. Sick and A. Weiss, *Z. Naturforsch., Teil B*, 1973, **28**, 168.
24 B. F. Walker and D. G. Hawthrone, *Trans. Faraday Soc.*, 1976, **63**, 166.